Coexpression of *neuronatin* splice forms promotes medulloblastoma growth

I-Mei Siu, Renyuan Bai, Gary L. Gallia, Jennifer B. Edwards, Betty M. Tyler, Charles G. Eberhart, and Gregory J. Riggins

Departments of Neurosurgery (I.-M.S., R.B., G.L.G., J.B.E., B.M.T., G.J.R.) and Pathology (C.G.E.), Johns Hopkins University School of Medicine, Baltimore, MD, USA

Medulloblastoma (MB) is the most common pediatric brain cancer. Several important developmental pathways have been implicated in MB formation, but fewer therapeutic targets have been identified. To locate frequently overexpressed genes, we performed a comprehensive gene expression survey of MB. Our comparison of 20 primary tumors to normal cerebellum identified *neuronatin* (*NNAT*) as the most frequently overexpressed gene in our analysis. *NNAT* is a neural-specific developmental gene with α and β splice forms. Functional evaluation revealed that RNA interference knockdown of *NNAT* causes a significant decrease in proliferation. Conversely, coexpression of both splice forms in *NNAT*-negative MB cell lines increased proliferation, caused a significant shift from G_1 to G_2/M, and increased soft agar colony formation and size. When expressed individually, each *NNAT* splice form had much less effect on these in vitro oncogenic predictors. In an in vivo model, the coexpression of both splice forms conferred the ability of xenograft formation to human MB cells that do not normally form xenografts, whereas a control gene had no effect. Our findings suggest that the frequently observed overexpression of both *NNAT* splice forms in MB enhances growth in this cancer. *Neuro-Oncology 10, 716–724, 2008 (Posted to Neuro-Oncology [serial online], Doc. 07-00234, August 13, 2008. URL http://neuro-oncology.dukejournals.org; DOI: 10.1215/15228517-2008-038)*

Keywords: medulloblastoma, neuronatin, oncogene

Received November 9, 2007; accepted April 1, 2008.

Address correspondence to Gregory J. Riggins, Johns Hopkins University, CRB II Rm. 257, 1550 Orleans St., Baltimore, MD 21231 USA (griggin1@jhmi.edu).

Medulloblastomas (MBs) are the most common pediatric solid tumor malignancy; however, the current therapeutic regimen involves radiation therapy, which can damage the developing brain. Therapies that target the genes involved in tumor formation might provide the means to enhance therapy for MBs without radiation, and perhaps increase survival while decreasing the debilitating side effects of treatment. Genetic alterations known to give rise to MBs include *MYC* and *MYCN* amplification, as well as *PTCH* mutations,[1] which occur in 5%–15% of patients. Recently, genomic amplification of *NOTCH2* and *OTX2* in MBs has been reported.[2,3] Despite these very important advances in understanding the pathological basis of MB growth, the known oncogenes are generally expressed in only a small percentage of MBs. This presents difficulties in developing a molecular target for most MBs. To identify commonly overexpressed MB genes and to gain insight into MB growth, we performed large-scale gene expression analyses and functionally evaluated candidate MB-related genes. Evidence, by in vitro functional assays and an in vivo model, supports our main hypothesis presented here that neuronatin (NNAT) stimulates malignant growth when both of its splice forms are expressed in MB.

Materials and Methods

Tissue Samples, DNA, RNA, and Cell Lines

Two snap-frozen MBs were purchased from the Duke University Brain Tumor Bank. Two autopsy specimens of normal cerebella from a 78-year-old male and a 21-year-old female with diabetes mellitus were obtained from the Brain Bank of the Alzheimer Research Cen-

ter at Duke University. Genomic DNA from MBs was isolated by CsCl centrifugation or the DNAeasy kit (Qiagen), Valencia, CA, USA. Total RNA was isolated by CsCl centrifugation or the RNAgents Total RNA Isolation kit (Promega, Madison, WI, USA). The MB cell lines used in this study were D283Med, D341Med, D425Med, D581Med, D721Med, Med-mhh1, MCD-1, and UW228.

Serial Analysis of Gene Expression

Serial Analysis of Gene Expression (SAGE) and Micro-SAGE were performed as previously described.[4,5] SAGE was performed using 1–100 μg of total RNA from two MBs, two normal cerebella, and four MB cell lines (D341Med, Med-mhh1, UW228-pLAPSN, and UW228-*NNAT*α+β) to obtain transcript profiles for various comparisons using a p-value < 0.01. An additional 18 MBs were made using the same procedure and have been previously reported by our laboratory.[6] The various comparisons of the transcript profiles for these SAGE libraries were performed using either the SAGE2000 software, version 4.5 (available upon request from the B. Vogelstein/K. Kinzler lab, Johns Hopkins University) or the Digital Gene Expression Displayer tool on the National Cancer Institute's SAGE Genie Web site (http://cgap.nci.nih.gov/SAGE). All expression profiles are posted and can be downloaded from SAGE Genie.

PCR and Real-Time PCR

Regular, semiquantitative, and real-time PCR was performed on a panel of MBs and normal tissues (primer sequences upon request) as described previously.[4,7]

RNA Interference–Mediated Knockdown

The following dicer RNA interference (RNAi) duplexes were obtained from Integrated DNA Technologies (Coralville, IA, USA): HSS.RNAIN005386.3.3, which targets the *NNAT*α splice form only; ACC U31767 and HSC.RNAI.N005386.3.5, which target both *NNAT*α and *NNAT*β (*NNAT*α+β) splice forms; and a randomized small interfering RNA (siRNA) control. One million D283Med cells were electroporated at 200 V for 25 ms (GenePulser, Bio-Rad, Hercules, CA, USA) with 5 μg of RNAi duplex.

Immunohistochemistry

A rabbit polyclonal antibody was designed against the C-terminus of human NNAT (Zymed/Invitrogen, Carlsbad, CA, USA), used to stain 5-μm sections of formalin-fixed, paraffin-embedded MBs, normal cerebella, and normal white matter at a dilution of 1:100, and visualized by the chromagen diaminobenzidine.[8]

Western Blotting

Cytoplasmic extracts were made using the NE-PER Nuclear and Cytoplasmic Extraction Reagent Kit (Pierce, Rockford, IL, USA) following the manufacturer's instructions. Twenty micrograms of protein were heated for 5 min with 2.5% β-mercaptoethanol/lithium dodecyl sulfate sample buffer (Invitrogen, Carlsbad, CA, USA) and loaded onto a 4%–12% NuPAGE Bis-Tris gel (Invitrogen). The gel was transferred to a polyvinyl difluoride membrane and probed according to standard procedures using the anti-NNAT antibody described above at a dilution of 1:400. Signals were visualized by the Pico SuperSignal chemiluminescent system (Pierce).

Generation of Cell Lines

The two splice forms of *NNAT*, α (Mammalian Gene Collection clone; National Institutes of Health, http://mgc.nci.nih.gov/) and β (cloned by PCR), were each cloned into the retroviral vector pLNCX2 (Clontech, Mountain View, CA, USA). Briefly, both constructs and a control vector containing alkaline phosphatase (pLAPSN) were transfected separately into the ecotropic packaging cell line QNX. Supernatants from these cultures were then used to infect the amphotrophic packaging cell line PT-67. Subsequent supernatants were collected from PT-67+*NNAT*α, PT-67+*NNAT*β, and PT-67+pLAPSN to infect MCD-1 and UW228 cells, resulting in four daughter cell lines (pLAPSN, *NNAT*α, *NNAT*β, and *NNAT*α+β) for each cell line. All infected cultures of PT-67, MCD-1, and UW228 cells were subsequently placed under selection by G418 antibiotic (1 μg/ml) to select stable virus producers. Expression of *NNAT* transcript and protein was confirmed by reverse transcriptase (RT)-PCR and Western blotting, respectively (data not shown).

Cell Cycle and Proliferation Analysis

To determine the effects of the different splice forms on the cell cycle, flow cytometry was performed. For each of the four daughter cell lines of MCD-1 and UW228 (described above), 1×10^6 cells were counted, washed twice with phosphate-buffered saline (PBS), fixed overnight in 70% ethanol at 4°C, stained with 1 ml propidium iodide (PI) mix (5 μg/ml PI in PBS, 20 μg/ml RNase A, 0.1% Triton X-100),[9] and then analyzed by flow cytometry. For continuous monitoring of D283Med cells postelectroporation, alamarBlue (Invitrogen) was used according to the manufacturer's instructions. Proliferation rates for the various infections were analyzed by Cell Counting Kit 8 (CCK-8; Alexis Biochemical Corp., Lausen, Switzerland) according to the manufacturer's instructions.

Soft-Agar Colony Assay

Anchorage-independent growth was assayed by plating 1×10^3 cells/ml of each of the daughter cell lines of MCD-1 and UW228 in 0.4% agar on a 0.8% agar base. Six weeks after the initial seeding, colonies were counted using a scored eyepiece.

In Vivo Tumorigenicity

Four million UW228-pLAPSN, UW228-NNATα+β, MCD1-pLAPSN, or MCD1-NNATα+β cells were injected in an equal volume of reduced-growth-factor Matrigel (BD Biosciences, San Jose, CA, USA) in a total volume of 200 µl subcutaneously in the flanks of 8-week-old female athymic nude mice (National Cancer Institute, Frederick, MD, USA). Eight weeks after injection, animals were sacrificed and any tumorlike tissue at the injection site was collected, fixed in 10% formalin for 24 h followed by 70% ethanol, and embedded in paraffin. Samples were sectioned at 5 µm, stained with hematoxylin and eosin per standard histopathological technique, and analyzed by a neuropathologist (C.G.E.).

Bioinformatics/Pathway Analysis

To identify pathways potentially regulated by NNAT overexpression, we used two different programs, WebGestalt[10] (Vanderbilt University; http://bioinfo.vanderbilt.edu/webgestalt) and Bibliosphere Pathway Analysis (Genomatix, Munich, Germany) to analyze the SAGE data. Both programs organize genes based on Gene Ontology categories, Biocarta pathways, or Kyoto Encyclopedia of Genes and Genomes (KEGG) biochemical pathways. The WebGestalt program performs a ratio of enrichment (R) calculation as well as the *p*-value calculation associated with this ratio when the input list is compared to a reference human set. The version of the Bibliosphere Pathway Analysis program we used identifies pathways and networks of pathways by literature mining.

Results

To find new genes or pathways activated in MB pathogenesis, we first compared the SAGE[4] transcript profiles of two MBs to those of normal cerebella, the site of origin for MBs. This revealed that these MBs express the neural developmental gene *NNAT* at very high levels. *NNAT* had been previously identified as up-regulated in MBs by subtractive hybridization screening as well.[11] We then compared the SAGE transcript profiles from an additional 18 MBs to those of the two cerebella and found that only *NNAT* transcription was up-regulated more than 10-fold in a majority (90%) of MBs, based on Bayesian statistics, with a *p*-value of 0.01. In this comparison, *NNAT* was the gene most induced compared to the normal controls. The *NNAT* transcript counts are shown in Table 1. Seventeen of 20 MBs had expression of *NNAT* greater than 1 in 10,000 transcripts, indicating that *NNAT* overexpression in MBs is a common event.

To confirm our transcript expression analysis results in a larger panel of MBs, we performed conventional PCR (Fig. 1A) and real-time PCR (data not shown) to determine the frequency and level of *NNAT*α+β overexpression in MBs. Both RT-PCR and real-time PCR of the MB panel and the 20 SAGE libraries showed that both *NNAT* splice forms are overexpressed at the RNA level in 90% (36 of 40) of MBs. We also confirmed NNAT protein expression in MBs by immunostaining MB sections and tissue arrays and found that 80% (57 of 72) of MBs were immunopositive for NNAT; although most of the immunoreactivity is cytoplasmic or membranous, in some tumor cells nuclear staining is present (Fig. 1B).

The PCR results indicated that the *NNAT*α splice form constituted the majority of *NNAT* expression in the tumors. In order to ascertain whether *NNAT*α was preferentially reexpressed in MBs, we performed semiquantitative PCR. We found that the higher the total *NNAT* expression as measured by SAGE transcripts, the more *NNAT*α is proportionally overexpressed (Fig. 1C).

Since *NNAT*, a neural development gene, was overexpressed in a high percentage of MBs at both the transcript and protein level, we next investigated whether it had a functional role in this cancer. To initially define the role of *NNAT* in MBs, we performed RNAi-mediated knockdown of either the *NNAT*α splice form only or *NNAT*α+β splice forms (Fig. 2), both of which resulted in a significant decrease (40%–50%) in growth compared to the scrambled RNAi negative control at 48 h after electroporation.

We then sought to determine whether *NNAT*α and/or *NNAT*β was capable of enhancing tumorigenicity when expressed in MB. We chose to use MB cell lines instead of cell lines such as NIH3T3 as the in vitro

Table 1. *NNAT* transcript counts in primary MBs as determined by SAGE

Sample	Tags per 200,000
MB1	2,244
MB2	892
MB3	701
MB4	472
MB5	388
MB6	317
MB7	158
MB8	78
MB9	71
MB10	53
MB11	46
MB12	44
MB13	44
MB14	41
MB15	29
MB16	23
MB17	23
MB18	17
MB19	6
MB20	0
Normal cerebellum 1	3
Normal cerebellum 2	0

MB, medulloblastoma.

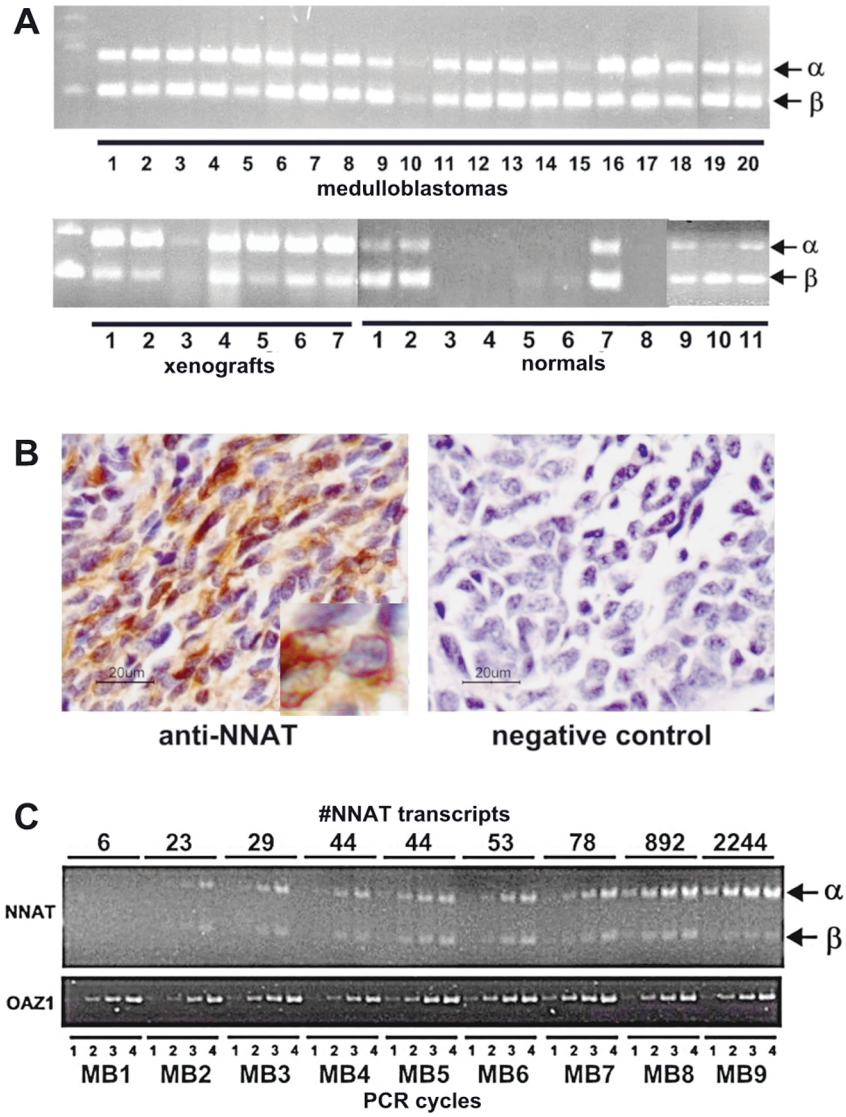

Fig. 1. *Neuronatin* (*NNAT*) is overexpressed in medulloblastoma (MB) tumors. (A) Reverse transcriptase–PCR was performed on a panel of MB resections (1–20; top lanes), xenografts, cell lines, and normal tissues (bottom lanes: lanes 1–3, cerebellum; 4, gray matter; 5, white matter; 6, caudate nucleus; 7, fetal brain; 8, total normal brain; 9 and 10, cerebellum; 11, fetal brain). *NNAT*α is present at levels equal to or higher than those of *NNAT*β in MBs, xenografts, and cell lines. In fetal brain and in cerebellum, *NNAT*β is present at levels equal to or higher than those of *NNAT*α. In the other normal brain structures we tested, both *NNAT* splice forms are absent. (B) Immunohistochemical staining of a primary MB with anti-NNAT (left) or without anti-NNAT (right). *NNAT* is overexpressed in MBs at the protein level and appears to localize in the membrane or cytoplasm in most cells, as shown in the inset, although some cells show a nuclear localization. Original magnification, ×100. (C) Semiquantitative PCR of MBs, which express a range of Serial Analysis of Gene Expression (SAGE) transcript levels (indicated above the corresponding set of PCRs for each tumor) performed at 24, 27, 30, and 33 cycles (indicated by 1, 2, 3, and 4, respectively, below gel). Higher overall *NNAT* expression correlates with reexpression of *NNAT*α.

model because we were going to perform gene expression analysis of these cell lines and believed that in order to interpret the results in the context of MB biology, it would be more appropriate to use MB cell lines. Additionally, the MB cell lines we used do not normally form in vivo xenografts, which meant that tumor formation might indicate tumor-promoting ability of *NNAT*. We created cell lines from parental MB cell lines MCD-1 and UW228, both of which do not express *NNAT*. Lines were made that express (1) *NNAT*α+β, (2) each splice form individually, and (3) pLAPSN (an alkaline phosphatase control gene). PI staining and flow cytometric analysis of these modified cell lines showed that *NNAT*α or *NNAT*β individually caused a small shift from G_1 to G_2/M, increasing the G_2/M. However, the presence of *NNAT*α+β caused a larger shift from G_1 to G_2/M of approximately 2-fold compared to control (Fig. 3A). In vitro growth of *NNAT*α, *NNAT*β, *NNAT*α+β,

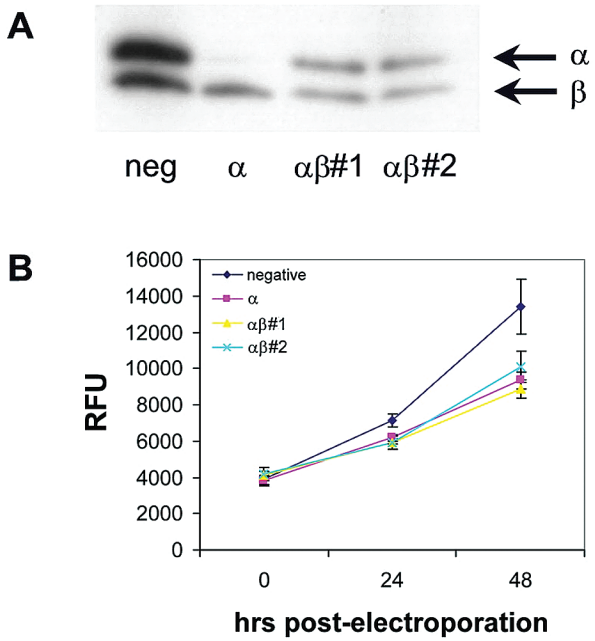

Fig. 2. RNA interference (RNAi)-mediated knockdown of *neuronatin* (*NNAT*) splice forms. (A) Western blot of D283Med cells 48 h postelectroporation of dicer-ready RNA interference duplexes targeting *NNAT*α only or *NNAT*α+β; equal amounts of protein were loaded per well. neg, scrambled RNAi negative control. (B) alamarBlue proliferation assay of D283Med cells after small interfering RNA electroporation. Knockdown of the *NNAT*α splice form alone or *NNAT*α+β splice forms results in a significant decrease in proliferation. Error bars represent variation in triplicate wells. RFU, relative fluorescence units.

and control was measured over 4 days. Again, the presence of *NNAT*α+β caused the largest increase in the rate of proliferation (~2-fold that of control), whereas either *NNAT*α or *NNAT*β alone exhibited only a modest increase in proliferation compared to the control pLAPSN (Fig. 3B). Similar effects of increased proliferation with both *NNAT* splice forms were observed in both the MCD-1 and UW228 background cell lines.

We then assayed the ability of these cell lines to grow in an anchorage-independent fashion, which is another indicator of the tumorigenic potential of transformed cells. Colonies formed in soft agar at a high rate only when *NNAT*α+β was present (19-fold that of pLAPSN), suggesting that both splice forms are necessary for anchorage-independent growth (Fig. 3C). In contrast, the presence of *NNAT*α or *NNAT*β separately did not induce highly significant soft agar colony formation, although cell lines expressing *NNAT*α did form more and larger colonies (~4-fold more colonies) than did the *NNAT*β- or pLAPSN-expressing cell lines (Fig. 3C). Not only did cell lines expressing *NNAT*α+β form significantly more soft agar colonies, but also these colonies were much larger, supporting the results of the proliferation assays (Fig. 3B). To ascertain the effect of *NNAT* on invasion and migration, we performed Matrigel invasion chamber assays and scratch assays, respectively, and the presence of *NNAT* did not affect tumor cell motility in either (data not shown). Our data so far are consistent with the hypothesis that expression of both *NNAT* splice forms promotes tumor growth by altering the cell cycle. *NNAT* may also help the tumor establish in certain microenvironments.

Increased colony formation in soft agar suggested that we should evaluate the ability of *NNAT*α+β to enhance tumor formation in an in vivo model. Neither of the MB cell lines MCD-1 and UW228 ordinarily grows as a xenograft when injected into nude mice.[9] In our studies, the UW228 cell line expressing the pLAPSN control also failed to form flank tumors in three of three mice, whereas the MCD-1 cell line failed to form tumors in mice regardless of whether it expressed pLAPSN or *NNAT*α+β. However, the UW228 cell line expressing *NNAT*α+β was able to form small subcutaneous tumors in three of three mice (Fig. 4A). Histologically, these tumors were consistent with the pathological definition of MBs; they were composed of embryonal cell that had pleomorphic nuclei and showed increased mitotic activity (Fig. 4B, arrows).

Given this evidence supporting a functional role in tumor formation, we sought to gain preliminary insight into the oncogenic signal promoted by *NNAT* overexpression. To find the pathway(s) potentially regulated by NNAT, as reflected by mRNA levels, we made SAGE libraries of UW228-pLAPSN and UW228-*NNAT*α+β. SAGE data analysis resulted in a list of 414 genes that were overexpressed in UW228-*NNAT*α+β compared to UW228-pLAPSN, using the parameters of p-values < 0.01 and increased expression by at least 3-fold. We then used this list of differentially expressed genes as the input genes for the WebGestalt pathway analysis software suite and for the Bibliosphere Pathway Analysis software (Table 2). Both software programs use Gene Ontology, Biocarta pathways, and KEGG biochemical pathways. We found several oncogenic pathways potentially associated with *NNAT* overexpression according to the analyses performed with the two different programs. These pathways are the phosphoinositide 3-kinase (PI3K) pathway, the mitogen-activated protein kinase (MAPK) pathway, the calcium signaling pathway, and various metabolic pathways. We also performed additional SAGE library comparisons of two *NNAT*-positive primary MBs versus one *NNAT*-negative MB and one low-*NNAT*-expressing primary MB. After identifying genes that were significantly (p-value < 0.05, at least 3-fold greater) overexpressed in the *NNAT*-positive population, we performed the same bioinformatic analyses using the WebGestalt program. Some of the pathways we identified as being significantly up-regulated in our *NNAT*-overexpressing in vitro model (p-value < 0.01) were also significantly up-regulated in the *NNAT*-overexpressing primary MBs with endogenous *NNAT* overexpression (Table 2), suggesting that these pathways are indeed regulated by *NNAT*. Pathway analysis by the WebGestalt program also found that the MAPK signaling pathway and the signaling pathway downstream of mTOR, a serine/threonine kinase that is the mammalian

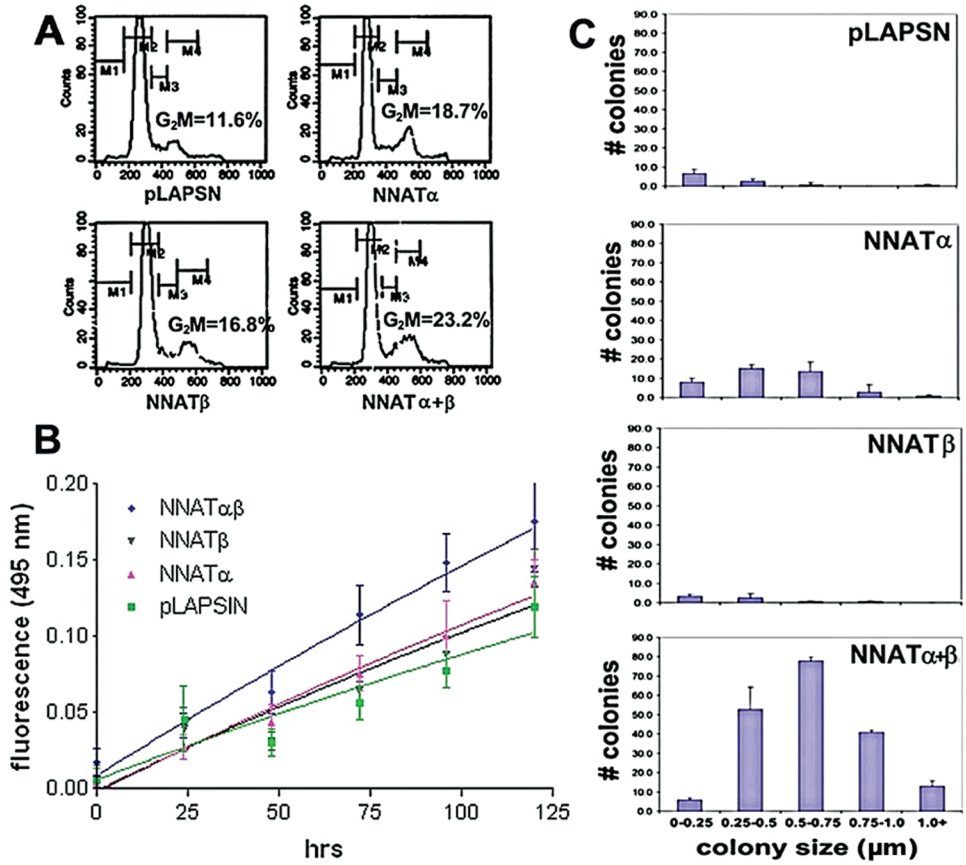

Fig. 3. Analysis of the growth properties of cells expressing *neuronatin* (*NNAT*) splice forms. (A) Expression of *NNAT*α+β causes a shift from G_1 to G_2M, whereas expression of *NNAT*α or *NNAT*β alone did not significantly alter cell cycle progression. (B) Growth curves of UW228 medulloblastoma (MB) cell lines expressing pLAPSN, *NNAT*α, *NNAT*β, and *NNAT*α+β. Cells expressing *NNAT*α and *NNAT*β grew at roughly similar rates, whereas the cell line expressing *NNAT*α+β grew at a significantly increased rate; cells expressing the control pLAPSN grew the slowest. A representative experiment is shown, with error bars representing the variation in triplicate wells. (C) Coexpression of *NNAT*α and *NNAT*β causes significant anchorage-independent growth in soft agar. UW228 MB cell lines expressing the control pLAPSN or *NNAT*β formed few colonies, which were mostly 0–0.25 μm in diameter. The expression of *NNAT*α slightly increased both the number and size of colonies formed, but the coexpression of *NNAT*α and *NNAT*β together caused a significant increase in both the number and size of soft agar colonies.

target of rapamycin, were both significantly up-regulated in our in vitro system, although not in the *NNAT*-positive MBs. This may perhaps be due to the high degree of heterogeneity of MBs and the lack of truly *NNAT*-negative primary MBs. There was an overlap in many of the pathways identified by both the WebGestalt program and the Bibliosphere Pathway Analysis program, although the latter identified additional pathways that may also be associated with *NNAT* overexpression. One of these included the insulin-signaling pathway, which is of particular interest because previous studies had demonstrated the role of *NNAT* in insulin secretion by the pancreas.[12]

Discussion

NNAT is an alternatively spliced gene whose two splice forms, *NNAT*α and *NNAT*β, are expressed during mouse development with a period of strong overlapping expression.[13,14] *NNAT*α appears first, followed later by *NNAT*β, but by birth *NNAT*α expression has been largely abated, leaving *NNAT*β as the predominant splice form.[14] The two splice forms differ by the absence of a small transmembrane domain in *NNAT*β, which in normal children and adults is present at only low levels.[15–17] The *NNAT* gene is located in the intron of a biallelically expressed, antisense transcript, bladder cancer-associated protein (*BLCAP*),[16] which we concluded was not directly involved in MB because it is not overexpressed in our MB SAGE libraries. It has also been shown that *BLCAP* is not involved in antisense regulation of *NNAT*.[16]

During development, *NNAT* expression is regulated by epigenetic modifications.[18–21] By virtue of its expression pattern during development, *NNAT* has been postulated to participate in the maintenance of segment identity in the mammalian hindbrain.[13] The two *NNAT* isoforms, α and β, have distinct patterns of expression during development,[14] suggesting that there is differential regulation between the two isoforms and that there

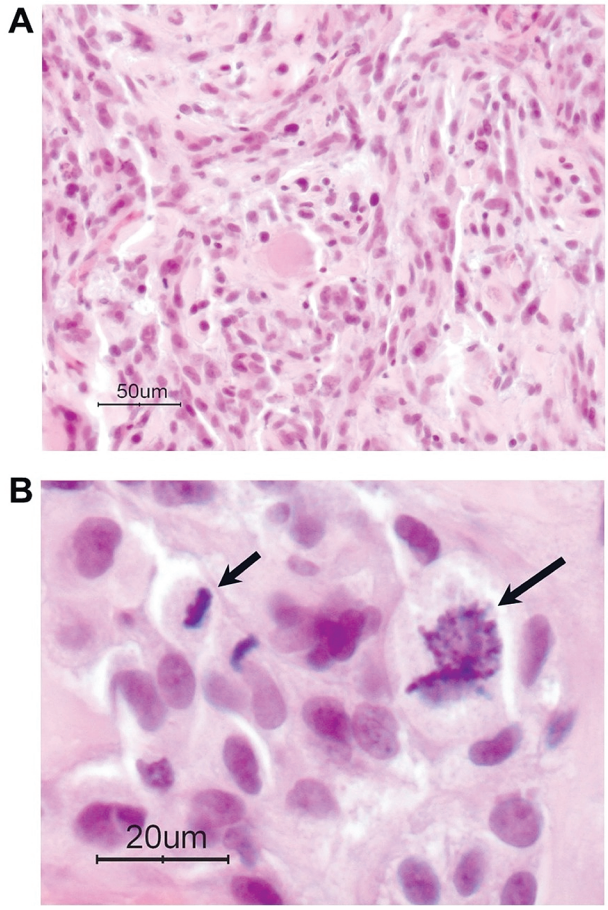

Fig. 4. Expression of *neuronatin* (*NNAT*) α and β splice forms in UW228 medulloblastoma cells induces subcutaneous tumor formation in the flanks of three of three athymic nude mice. (A) Hematoxylin- and eosin-stained sections of a xenograft expressing *NNAT*α+β showing a moderately cellular tumor with pleomorphic nuclei. (B) Hematoxylin- and eosin-stained sections of a xenograft expressing *NNAT*α+β with increased proliferation of malignant cells as indicated by the presence of mitotic figures (arrows).

are possibly different roles played by the two isoforms during development. Interestingly, *NNAT* is a known target of *NeuroD1* (neurogenic differentiation 1),[12] which itself has been shown to be involved in granule cell precursor differentiation,[22] and is overexpressed in 15 of the 21 MB SAGE libraries constructed in our lab (posted at http://cgap.nci.nih.gov/SAGE). *NNAT* is expressed in the granule cell layer of newborn mouse cerebellum,[19] as is *NeuroD1*.[22] So far, there is no direct evidence that the *NNAT* is either directly or indirectly activated by *NeuroD1* in MBs, but these findings taken together suggest this is a hypothesis worth testing.

NNAT had a dramatic increase in transcription compared to adult brains in our expression survey. It also has an active role in neural development, which is consistent with known oncogenes and tumor suppressors for MB. We found that high levels of total *NNAT* expression in MBs are due mostly to increased expression of *NNAT*α, but is also associated with some increased expression of *NNAT*β (Fig. 1C). This finding, and the developmental pattern of expression of the *NNAT* splice forms, suggests that both splice forms might be needed for the tumorigenic potential of *NNAT*. This was supported by our demonstration of the significant increase in anchorage-independent growth and a shift from G_1 to G_2M only with the presence of both *NNAT* splice forms. Additionally, our findings that *NNAT*α is the predominant splice form in MBs and that knockdown of endogenous *NNAT*α alone or with endogenous *NNAT*β simultaneously causes a decrease in proliferation, suggests that it is specifically the presence of *NNAT*α that is primarily responsible for the tumor-promoting behavior of this gene.

Pathway analysis of the isogenic cell line model we created revealed that known cancer-related pathways such as the PI3K and MAPK pathways are up-regulated in *NNAT*α+β-expressing cells, further supporting the potential role of *NNAT* in promoting tumorigenicity. Previous studies have shown that some of these pathways are up-regulated in MBs, including the PI3K/Akt pathway.[23] Interestingly, known oncogenes such as *H-RAS* and *MAPK1* were significantly up-regulated in UW228-*NNAT*α+β cells (p-value < 0.01; 3.5-fold and 18.7-fold, respectively). From data mining of transcript profiles on the National Cancer Institute's SAGE Genie database, we observed that *NNAT* is up-regulated in MB cells that are resistant to 4-hydroperoxycyclophosphamide, which is commonly used to treat MBs. *NNAT* has previously been linked to tamoxifen resistance in mammary carcinoma xenografts;[24] both of these findings suggest that NNAT may have a role in chemotherapeutic drug resistance. Unfortunately, the gene expression analysis we performed does not reveal how NNAT might promote drug resistance, but functional studies of the genes induced by NNAT might resolve the question of whether NNAT is directly involved in promoting chemoresistance.

We have accumulated evidence that *NNAT* expression promotes tumorigenic growth of MB cells, but we have not identified any genomic alterations that pathologically trigger its expression in cancer. A screen of the coding region of *NNAT* in 20 primary MBs failed to identify any mutations, suggesting that mutations in *NNAT* are rare. We cannot exclude the possibility that increased *NNAT* expression is triggered by upstream signaling, promoter mutations, epigenetic changes, or any combination of these. A report of imprinting at the *NNAT* locus prompted us to investigate methylation changes at the presumed *NNAT* promoter, but this failed to yield conclusive evidence of this potentially important means of expression reactivation.

Although our studies are limited to *NNAT*'s role in MB, its involvement in some other cancers cannot be excluded. Using the SAGE Genie database, we found little or no expression of *NNAT* in 23 classes of normal tissue. However, we found that *NNAT* is also overexpressed, with levels of more than 3 per 10,000 transcripts, in ependymomas, a mesothelioma, and a rhabdomyosarcoma. Other groups have demonstrated

Table 2. Pathways significantly up-regulated in *NNAT*-overexpressing populations

Biocarta/KEGG Pathway	*p*-Value (UW228αβ)	*p*-Value (*NNAT*-Positive Primary MBs)
Lysine degradation	0.0003	0.00031
Purine metabolism	0.00054	0.0017
Rho cell motility signaling pathway	0.0018	0.0075
Focal adhesion	0.0019	0.015
Erk and PI3K are necessary for collagen binding in corneal epithelia	0.0025	0.005
Butanoate metabolism	0.004	0.0088
Pyrimidine metabolism	0.0053	0.0063
Long-term potentiation	0.0076	0.0076

Abbreviations: *NNAT*, *neuronatin*; KEGG, Kyoto Encyclopedia of Genes and Genomes; MB, medulloblastoma; PI3K, phosphoinositide 3-kinase.

a correlation between *NNAT* overexpression and poor prognosis of non-small-cell lung cancer.[25] A recent report indicates that *NNAT* is expressed as a result of acquired tamoxifen resistance in breast cancer xenografts.[24]

To the best of our knowledge, this is the first report characterizing *NNAT* as having a potential functional role in cancer. Our in vitro and in vivo results indicate that the increased expression of the *NNAT*α splice form is pathological and that its coexpression with *NNAT*β causes increased proliferation of MBs. The high expression and proportion of *NNAT*α in total *NNAT* expression in MBs correlates with that seen during neural development (Fig. 1A).[14] Previous rat developmental studies have shown that the coexpression of both splice forms, with *NNAT*α predominantly expressed relative to *NNAT*β, coincides with a time in gestation of neuroepithelial proliferation and differentiation,[14] suggesting that the *NNAT* splice forms interact during development. This is consistent with our findings that the combined presence of *NNAT*α+β caused an increase in proliferation, anchorage-independent growth, and tumor formation in vivo. Furthermore, our expression analysis suggests that coexpression of *NNAT*α+β may regulate both known cancer-related pathways as well as pathways known to be regulated by *NNAT* but not previously described in MBs or other cancers. Up-regulated metabolic pathways in response to NNAT also suggest additional approaches to evaluate for MB therapy.

NNAT is approximately 50% homologous to the class of proteolipids that are regulatory subunits of ion channels.[17] If NNAT does indeed act to regulate ion channels, one mechanism of NNAT action may involve the formation of a heterodimer or multimer comprising the *NNAT*α+β splice forms in order to exert this regulation in MBs. We have demonstrated that knockdown of *NNAT*α results in decreased proliferation and that only expression of *NNAT*α+β simultaneously results in the highest increase in proliferation; these findings suggest that the two *NNAT* splice forms may interact, although physical interaction of the two splice forms has not been addressed by these experiments.

We conclude that *NNAT* is one of the most commonly overexpressed genes in MBs, that it acts in an oncogenic fashion, and that the coexpression of both *NNAT* splice forms is necessary for significant increase in proliferation. The ability of coexpressed *NNAT*α+β to promote tumor formation in cells devoid of tumor-forming capacity also hints at a critical role for this gene in MB progression.

Acknowledgments

We thank Stephen Baylin, J. Keith Killian, and James G. Herman for helpful discussion and insights about methylation; Ashani Weeraratna, Vinay Prabhu, and Kevin Becker for helpful discussion regarding bioinformatic pathway analysis of the SAGE data; John Silber, William Freed, and Torsten Pietsch for the UW228, MCD-1, and Med-mhh1 cell lines, respectively; and Brenda J. Raymond for her assistance in the preparation of the manuscript. This work was supported by funds from National Institutes of Health grant NS052507, the American Brain Tumor Association, and the Virginia and D.K. Ludwig Fund for Cancer Research. G.J.R. is the recipient of the Irving J. Sherman M.D. Research Professorship.

References

1. Raffel C, Jenkins RB, Frederick L, et al. Sporadic medulloblastomas contain PTCH mutations. *Cancer Res*. 1997;57:842–845.
2. Fan X, Mikolaenko I, Elhassan I, et al. Notch1 and notch2 have opposite effects on embryonal brain tumor growth. *Cancer Res*. 2004; 64:7787–7793.
3. Boon K, Eberhart CG, Riggins G. Genomic amplification of *orthodenticle homologue 2* in medulloblastomas. *Cancer Res*. 2005;65: 703–707.
4. Velculescu VE, Zhang L, Vogelstein B, Kinzler KW. Serial analysis of gene expression. *Science*. 1995;270:484–487.
5. St Croix B, Rago C, Velculescu V, et al. Genes expressed in human tumor endothelium. *Science*. 2000;289:1197–1202.
6. Boon K, Edwards JB, Siu IM, et al. Comparison of medulloblastoma and normal neural transcriptomes identifies a restricted set of activated genes. *Oncogene*. 2003;22:7687–7694.
7. Loging WT, Lal A, Siu IM, et al. Identifying potential tumor markers and antigens by database mining and rapid expression screening. *Genome Res*. 2000;10:1393–1402.
8. Siu I-M, Pretlow TG, Amini SB, Pretlow TP. Identification of dysplasia in aberrant crypt foci. *Am J Pathol*. 1997;150:1805–1813.
9. Stearns D, Chaudhry A, Abel TW, et al. c-myc overexpression causes anaplasia in medulloblastoma. *Cancer Res*. 2006;66:673–681.
10. Zhang B, Kirov S, Snoddy J. WebGestalt: an integrated system for exploring gene sets in various biological contexts. *Nucleic Acids Res*. 2005;33:W741–W748.
11. Yokota N, Mainprize TG, Taylor MD, et al. Identification of differentially expressed and developmentally regulated genes in medulloblastoma using suppression subtraction hybridization. *Oncogene*. 2004;23:3444–3453.
12. Chu K, Tsai MJ. Neuronatin, a downstream target of BETA2/NeuroD1 in the pancreas, is involved in glucose-mediated insulin secretion. *Diabetes*. 2005;54:1064–1073.
13. Wijnholds J, Chowdhury K, Wehr R, Gruss P. Segment-specific expression of the *neuronatin* gene during early hindbrain development. *Dev Biol*. 1995;171:73–84.
14. Joseph R, Dou D, Tsang W. Neuronatin mRNA: alternatively spliced forms of a novel brain-specific mammalian developmental gene. *Brain Res*. 1995;690:92–98.
15. Usui H, Morii K, Tanaka R, et al. cDNA cloning and mRNA expression analysis of the human neuronatin. *J Mol Neurosci*. 1997;9:55–60.
16. Evans HK, Wylie AA, Murphy SK, Jirtle RL. The neuronatin gene resides in a "micro-imprinted" domain on human chromosome 20q11.2. *Genomics*. 2001;77:99–104.
17. Dou D, Joseph R. Cloning of human *neuronatin* gene and its localization to chromosome-20q11.2–12: the deduced protein is a novel "proteolipid." *Brain Res*. 1996;723:8–22.
18. Kagitani F, Kuroiwa Y, Wakana S, et al. *Peg5/neuronatin* is an imprinted gene located on sub-distal chromosome 2 in the mouse. *Nucleic Acids Res*. 1997;25:3428–3432.
19. Kikyo N, Williamson CM, John RM, et al. Genetic and functional analysis of *neuronatin* in mice with maternal or paternal duplication of distal chr 2. *Dev Biol*. 1997;190:66–77.
20. John RM, Aparicio SAJR, Ainscough JF-X, et al. Imprinted expression of *neuronatin* from modified BAC transgenes reveals regulation by distinct and distant enhancers. *Dev Biol*. 2001;236:387–399.
21. Ruddock NT, Wilson KJ, Cooney MA, et al. Analysis of imprinted messenger RNA expression during bovine preimplantation development. *Biol Reprod*. 2004;70:1131–1135.
22. Miyata T, Maeda T, Lee JE. NeuroD is required for differentiation of the granule cells in the cerebellum and the hippocampus. *Genes Dev*. 1999;13:1647–1652.
23. Hartmann W, Digon-Sontgerath B, Koch A, et al. Phosphatidylinositol 3′-kinase/AKT signaling is activated in medulloblastoma cell proliferation and is associated with reduced expression of PTEN. *Clin Cancer Res*. 2006;12:3019–3027.
24. Becker M, Sommer A, Kratzschmar JR, et al. Distinct gene expression patterns in a tamoxifen-sensitive human mammary carcinoma xenograft and its tamoxifen-resistant subline MaCa 3366/TAM. *Mol Cancer Ther*. 2005;4:151–168.
25. Uchihara T, Okubo C, Tanaka R, et al. Neuronatin expression and its clinicopathological significance in pulmonary non-small cell carcinoma. *J Thorac Oncol*. 2007;2:796–801.